Chapter

Transient Thermal Analysis of a Magnetorheological Knee for Prostheses and Exoskeletons during Over-Ground Walking

Rafhael Milanezi de Andrade, André Palmiro Storch, Lucas de Amorim Paulo, Antônio Bento Filho, Claysson Bruno Santos Vimieiro and Marcos Pinotti

Abstract

Proper knee movement is essential for accomplishing the mobility daily tasks such as walking, get up from a chair and going up and down stairs. Although the technological advances in active knee actuators for prostheses and exoskeletons to help impaired people in the last decade, they still present several usage limitations such as overweight or limited mechanical power and torque. To address such limitations, we developed the Active Magnetorheological Knee (AMRK) that comprises a Motor Unit (MU), which is a motor-reducer (EC motor and Harmonic Drive) and a MR clutch, that works in parallel to a magnetorheological (MR) brake. Magnetorheological fluids, employed in the MR clutch and brake, are smart materials that have their rheological properties controlled by an induced magnetic field and have been used for different purposes. With this configuration the actuator can work as a motor, clutch or brake and can perform similar movements than a healthy knee. However, the stability, control, and life of magnetorheological fluids critically depend on the working temperature. By reaching a certain temperature limit, the fluid additives quickly deteriorate, leading to irreversible changes of the MR fluid. In this study, we perform a transient thermal analysis of the AMRK, when it is used for walking over-ground, to access possible fluid degradation and user's discomfort due overheating. The resulting shear stress in the MR clutch and brake generates heat, increasing the fluid temperature during the operation. However, to avoid overheating, we proposed a mode of operation for over-ground walking aiming to minimize the heat generation on the MR clutch and brake. Other heat sources inside the actuator are the coils, which generate the magnetic fields for the MR fluid, bearings, EC motor and harmonic drive. Results show that the MR fluid of the brake can reach up to 31°C after a 6.0 km walk, so the AMRK can be used for the proposed function without risks of fluid degradation or discomfort for the user.

Keywords: magnetorheological fluid, magnetorheological actuator, thermal analysis, prosthesis, exoskeleton

1. Introduction

The gait is severely affected by lower-limb amputation and neuromotor diseases and to compensate the lost limb or impaired legs additional movements are required [1]. Walking and other daily activities, such as going up and down stairs, getting up and sitting down, can be severely impaired, reducing the mobility of the patient [2]. Over the years, researchers seek to develop suitable actuators for assistive lower-limb devices such as prosthesis and exoskeletons [3, 4]. In general, this kind of actuators can be divided into three major groups: passive, semi-active, and active [5, 6]. Passive devices do not require a power source for operation, they are designed for each type of application and do not allow performance adjustments [6]. Semi-active devices only dissipate energy through controllable dampers [7]. Active-type devices, on the other hand, are capable of supplying and dissipating energy in a controlled way [6, 8, 9]. Despite the disadvantages of semi-active and passive prostheses, the number of active prostheses is still small and only the Power Knee™ (PK, Ossur, Iceland) is available on the market. In addition, exoskeleton knee actuators still need to be improved to properly reproduce the knee gait kinematics for low energy consumption. Filho et al. [10], Garcia et al. [11], and Martinez-Villalpando and Herr [6] propose the use of linear actuators with a serial elastic element (SEA) between the femur and the tibia. This configuration has characteristics such as impact tolerance, low mechanical output impedance and passive storage of mechanical energy [12, 13]. However, they are heavy devices with high energy consumption, making it difficult to be used in prostheses or exoskeletons [9, 14].

On the other hand, magneto-rheological fluids (MR) are colloidal solutions composed by up to 50% of their volume of magnetically polarized micro particles mixed with an inert oil, usually mineral-based or silicone-based [15]. When the fluid is subjected to an external magnetic field, its particles begin to form columnar structures parallel to the magnetic flux lines; this behavior changes the rheological properties of the fluid, such as yield stress and others, in a reversible and proportional way to the induced magnetic field [16]; the response time is in order of milliseconds [17]. Due to these characteristics, MR fluids are used to develop devices for many applications in engineering and industry: vehicle suspensions [18], clutches [19], brakes [20], structural vibration damping [21], intelligent prosthesis [5, 22–24] and others. MR devices usually present low energy consumption and high torque-to-weight ratio [25, 26], which is important to increase the energy efficiency and reduce the weight of prostheses and exoskeletons' actuators [27].

Although the advances in actuators technology, the active actuators used in robotic devices are still heavy and bulky [28], and the passive and semi-active ones cannot properly reproduce the movement of a healthy knee. To address the shortcomings of the knee actuators, we developed the Active Magneto-Rheological Knee (AMRK) [29, 30]. The actuator employs a motor-unit (MU), composed by an EC 60 flat motor (Maxon Motors, Switzerland), harmonic drive CSG-14-100-2a (Harmonic Drive AG, Germany) and MR clutch, that works in parallel to a MR Brake. With this configuration the actuator has multifunctional working conditions and can reproduce movements similar to a healthy knee with low energy consumption [25, 26]. The system is assembled in a lightweight and compact structure and can be used as a prosthetic knee, a knee actuator for exoskeletons and in robotic functions [30].

The MR Clutch and MR Brake of the AMRK present multi-disc configuration to improve the torque-to-mass ratio and compactness. With this configuration, the systems can work in full-slip and non-slip conditions. In the full-slip regime, there is a relative movement between the input and output and the torque is transmitted by the shear stress of the MR fluid [31], which is responsible for high heat generation. When in non-slip condition, there is no relative movement between the input

and output and the system works as a solid unit [32]. In this case, the heat generation is due just by Joule effect on the coil. The properties of the MR fluid strongly depend on the temperature, for this reason, the fluid shows different performances with the temperature variation [33]. The viscosity of the fluid changes with temperature variation, which results in a change in its shear stress. Moreover, MR fluids use additives to decrease sedimentation and increase the dispersion of particles, and such additives are also sensitive to temperature variation, some of it decompose when reaching about 100°C [34]. Moreover, cyclic operation under high and low temperatures can lead to irreversible changes in the MR fluid. It can run-out its rheological properties, leading to uncontrolled shear stress due to the influence of material agglomeration under magnetic field conditions [33]. Since high temperature deteriorates the MR fluid, the full-slip operation is the most critical working condition for the MR clutch and MR brake [35]. Some works in the literature present methodologies to evaluate how these properties change with temperature [36]. Chen et al. [33] proposed an experimental setup to evaluate an MR transmission under different temperatures, obtaining a set of torque and temperature curves with different current inputs. Zipster et al. [37] proposed an experimental setup that analyzes the MR fluid in flow mode, under different temperatures. Wang et al. [34] made a complete characterization of the MR fluid under different temperatures. Here we present a transient thermal analysis of the AMRK under over-ground working conditions to evaluate if the heat generation can deteriorate the MR fluid or be dangerous for the user. Since the full-slip operation increases heat production, we proposed an operating mode for the AMRK that minimizes the heat dissipation on the MR clutch and brake to avoid high working temperatures.

2. The active MR knee

The AMRK configuration is presented in **Figure 1**. The system consists of a motor unit (MU) (EC 60 flat motor, harmonic reducer CSG-14-100-2a and MR clutch) mounted in parallel to an MR brake, and can work as a motor, clutch and brake. This configuration allows the actuator to be controlled independently by the MU or by the brake MR, exploring thereby the advantages of each subsystem. The device is supported by two main structures: The external structure connects to the upper part of the prosthesis/exoskeleton, the internal one connects to the lower part of the prosthesis/exoskeleton through adapters. A pair of thin section bearings allows relative movement between the external and internal structures. The structures are made of 7075 aluminum alloy [5], as shown in **Figure 1(a)**. **Figure 1(b)** displays the configuration of the MR clutch and MR brake. The dynamic model of the AMRK is presented in **Figure 1(c)**, and the proposed actuator operating modes for over-ground walking are shown in **Figure 1(d)**.

The MR brake is housed between the external and internal structures and dissipates energy just when the knee joint should exert negative work during over-ground walking, operating mode I in **Figure 1(d)**. The MR brake is designed with a multi-disc configuration and hollow iron core to reduce mass and increase torque capacity [38], as displayed in **Figure 1(b)**. The output disks are connected to the aluminum cover, which is attached to the external structure of the actuator. The output disks are assembled interlayered with the input disks, which are attached to the iron core that is coupled to the internal structure. The MR fluid fills the space between disks. The magnetic field induced by the coil controls the yield stress of the MR fluid; in this way, the MR fluid can behave as a semi-solid or a Newtonian fluid depending on the action of the magnetic field. Consequently, the resistive torque of the brake is controlled by the input current on the brake coil [39].

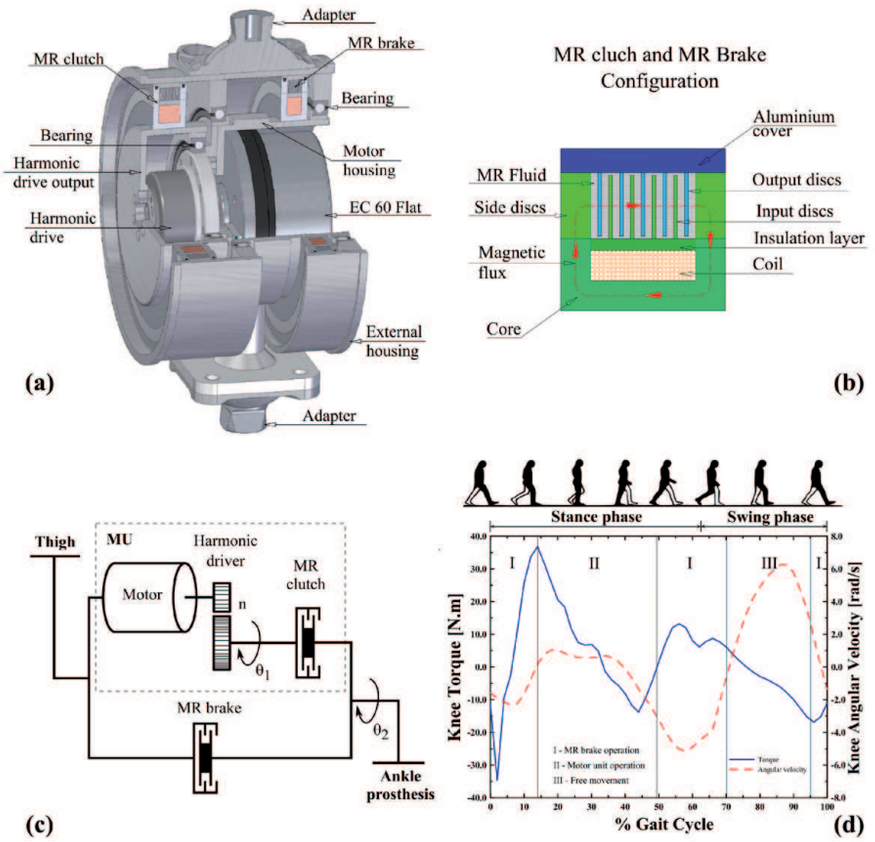

Figure 1.
The AMRK configuration and operation modes. (a) Cutaway view of the actuator. (b) configuration of the MR clutch and MR brake. (c) Dynamic model of the system. (d) Operating mode for over-ground walking used in the transient thermal analysis.

Active torque of the AMRK is required just when the knee exerts positive work, operating mode II in **Figure 1(d)**, and it is produced by the MU that comprises an EC motor, a harmonic drive (HD) and an MR clutch. The motor and HD stators are attached to the internal structure and the HD output is connected to the iron core of the MR clutch. The MR clutch has the same working principle as the MR brake, that is, when the magnetic field is activated, the MR fluid yield stress increases and prevents the relative movement between input and output disks. Thus, the torque produced by the motor-reducer is transferred to the external structure of the actuator controlled by the input current on the clutch coil. During swing phase, the knee rotates freely achieving high angular velocity. It can be accomplished by the AMRK as long as the MU is deactivated and the MR brake exerts low resistive torque to stabilize the joint, operating mode III in **Figure 1(d)**.

The torque supported by the MR brake and clutch follows the shear equation of a fluid between disks with relative angular movement [40], as shown below:

$$T = \int_{ri}^{ro} \tau_{MR} r_D dA \tag{1}$$

where τ_{MR} is the shear stress of the MR fluid, r_D is the radius of the disks, and A is the effective contact area between disks and MR fluid. The contact area can be described in terms of the number of gaps (N) filled by the MR fluid, and the internal (r_i) and external (r_o) radii of the disks. In addition, MR fluids behave like an ideal plastic fluid or Bingham plastic when subjected to magnetic field. Then the previous equation can be rewritten as:

$$T = 2N\pi\left[\frac{\tau_Y}{3}\left(r_o^3 - r_i^3\right) + \frac{\omega\mu_{MR}}{4h}\left(r_o^4 - r_i^4\right)\right] \tag{2}$$

where τ_y is the yield stress of the MR fluid, which is a function of the magnetic field strength and can be obtained from the manufacturer's catalog, μ_{MR} is the MR fluid viscosity, h is the gap thicknesses and ω is the angular velocity of the disks.

As the magnetic circuit is composed by a set of elements in series, the magnetic flux is uniform throughout the circuit [41]. As the desired value for the magnetic flux density in the MR fluid area (B_{MR}) is a design parameter, the magnetic flux can be described as follows:

$$\varphi = \pi\left(r_o^2 - r_i^2\right)B_{MR} \tag{3}$$

Similarly, the magnetic flux of a given circuit can also be described as a function of the number of coil's turns (N_b), the current (I) and the equivalent reluctance of the circuit (R_{eq}) [41]:

$$\varphi = \frac{N_b I}{R_{eq}} \tag{4}$$

It worth noting that Eqs. (3) and (4) are just valid as long as there is no magnetic saturation in any elements of the magnetic circuit.

Eqs. (1)–(4) are used to construct a parametrized model to optimize the design variables (see [5]) for more details). **Table 1** presents the optimized value of the design variables after optimization process.

Variable	Optimal Value	
	MR Brake	MR Clutch
T [N m]	35.0	55.4
r_o [mm]	54	
r_i [mm]	48.5	
N [gaps]	14	20
B_{MR} [T]	0.45	0.50
I [A]	2.1	1.8
N_t [turns]	164	226
τ_y [kPa]	27.3	30.3
R_c [ohm]	4.34	6.05
P [W]	19.2	19.6
M [kg]	0.37	0.46

Table 1.
MR brake and MR clutch variables.

3. Thermal model of the actuator

In this section we present the procedure adopted to build the thermal model for the AMRK to carry out a transient temperature simulation across a long walk over the ground. We set up a model for each element that comprises the actuator: EC motor, harmonic drive, MR clutch, MR brake, bearings and housing. The detailed method used is described in the following subsections.

3.1 Motor-reducer model

According to Maxon's Key Information for DC and EC motors [42], the losses of efficiency in the motor are divided into losses due to friction, P_{mec}, and due to the Joule effect, P_{J}, of the winding, which has resistance R_{a}. The energetic balance can be treated as:

$$P_{el} = P_{mec} + P_J \tag{5}$$

where P_{el} is the electrical power of the motor. The dissipation of power due Joule effect is given by:

$$P_J = R_a \cdot I_a^{\,2} \tag{6}$$

where I_{a} is the input current in the motor armature.

The thermal properties of the motor are given by the supplier catalog. We considered the EC 60 flat model 411,678 for the analysis. The temperature of the motor housing can be predicted when the free surfaces are submitted to air as in [43]:

$$P_J = \frac{T_S - T_\infty}{R_{th2}} \tag{7}$$

where T_{S} is the surface temperature, T_∞ is the environment temperature (25°C), and R_{th2} is the thermal resistance between the surface and the environment, which is given by the supplier catalog, and can also be described by the following equation [43]:

$$R_{th2} = \frac{1}{h_{comb} A_S} \tag{8}$$

where h_{comb} is the combined heat transfer coefficient for convection and radiation and A_{S} is the heat transfer surface area. By rearranging Eq. (8), and considering the motor assembled in a plastic plate to reproduce the standard cooling conditions, as described in [44], the coefficient h_{comb} = 1.72x10E-5 W/(mm^2 °C) is obtained.

In order to validate the EC 60 motor thermal model to be used in the actuator, a transient simulation of the motor's temperature is shown in **Figure 2**. The external surface of the motor reaches a maximum temperature of 51.12°C in about 7200 s, which is very close to the temperature obtained by the Eq. (7) (51.15°C), thereby validating the used method.

As previously described, the motor is used just when positive work of the knee joint is required. For intermittent work, the supplier recommends using the average input current, I_{RMS}, in the motor armature during the cycle operation. The input current variation for the proposed working modes (**Figure 1(d)**) is presented in **Figure 3**.

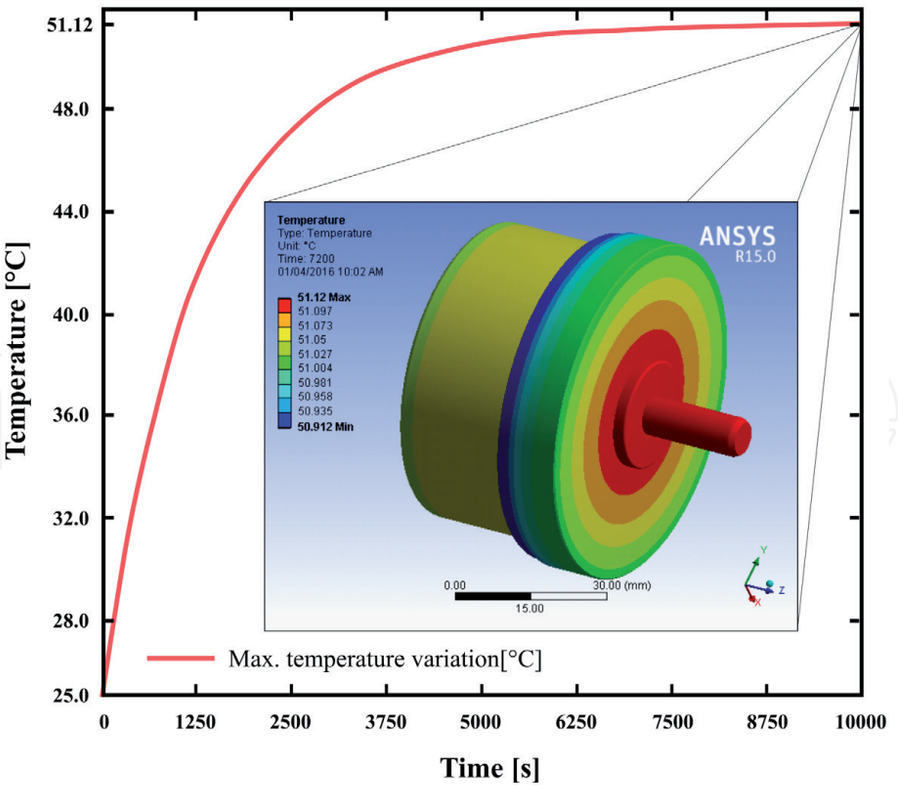

Figure 2.
Simulation of the motor's external temperature in nominal operating conditions. The highlighted color map represents the steady state temperature of the motor's surface.

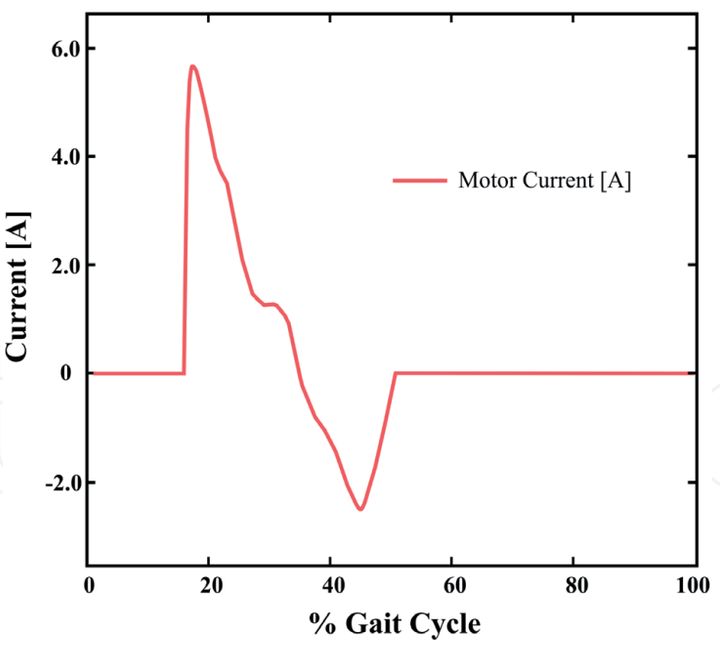

Figure 3.
Input current in the motor armature during the gait cycle.

We carried out a simulation considering the input current in the motor for the intermittent operating condition due to the gai cycle. A constant temperature of 28.86°C was obtained after 2 hours.

Regarding the harmonic drive, the heat generation (P_{HD}) occurs basically due friction between its movable parts and it can be calculated as follows:

$$P_{HD} = \tau_f \omega N \tag{9}$$

where τ_f is the friction torque that can be gathered from the supplier datasheet (Harmonic Drive AG, Germany), and ω is the angular velocity of the knee joint, as shown in **Figure 1(d)**, and N is the HD reduction ratio (N = 100). The presented intermittent working conditions for the CSG-14-100-2a, results in a RMS heat generation of 1.04 W.

3.2 MR clutch and MR brake

The proposed operating modes for the AMRK during over-ground walking consider that the MR clutch works in non-slip condition when the magnetic field is activated and in full-slip condition when no transmitting torque is required. Since the power is dissipated as heat in the MR fluid region and it is a function of the torque and the angular velocity between disks, the MR clutch does not present heat generation in the fluid area. On the other hand, the MR brake is always subjected to the full-slip operation and generates heat in the MR fluid region. However, the brake just works when braking torque or joint stabilization is required, thereby minimizing the heat generation.

The fluid used in the prototype is the MRF-140 CG, which has a recommended working temperature between −40°C and 130°C, according to the manufacturer. However, Chen et al. [33] reported that there is a reduction in the yield stress of the MR fluid at temperatures around 100°C, due to the deterioration of some additives. For this reason, it is safe to limit the working temperature of the MR fluid to 100°C. Heat generation due to the sliding condition is given by [35]:

$$\dot{\Phi}_d = \frac{T\omega}{V_f} \tag{10}$$

where $\dot{\Phi}_d$ is the volumetric generation of heat in the fluid, T and ω are the torque and angular velocity of the knee, respectively, and V_f is the volume of the fluid.

The loss of electrical power due to the Joule effect on the coil can be written as [35].

$$\dot{\Phi}_C = \frac{I^2 R_C}{V_C} \tag{11}$$

where $\dot{\Phi}_C$ is the volumetric generation of heat in each coil, I is the electric current in the coil, R_C is the resistance of the coil, and V_c is the volume of the coil. The electrical current variation in the MR clutch/brake coils during the gait cycle for the proposed working modes is shown in **Figure 4**.

The other components to be modeled are the bearings and the convection coefficient on the free surfaces of the actuator. According to the NTN bearing catalog [45], bearing friction becomes a cause of heat generation that must be considered. Eq. (12) describes the heat generation applied to the bearings.

$$\dot{\Phi}_B = \frac{1.05\times10^{-4}\,\mu P d \Delta\omega}{2V_B} \tag{12}$$

where $\dot{\Phi}_B$ is the volumetric heat generation in the bearing, μ is the friction coefficient given by the manufacturer's datasheet, P is the load to which the bearing is subjected, ω is the knee joint angular velocity, d is the inner diameter of the bearing, and V_B is the volume of the bearing.

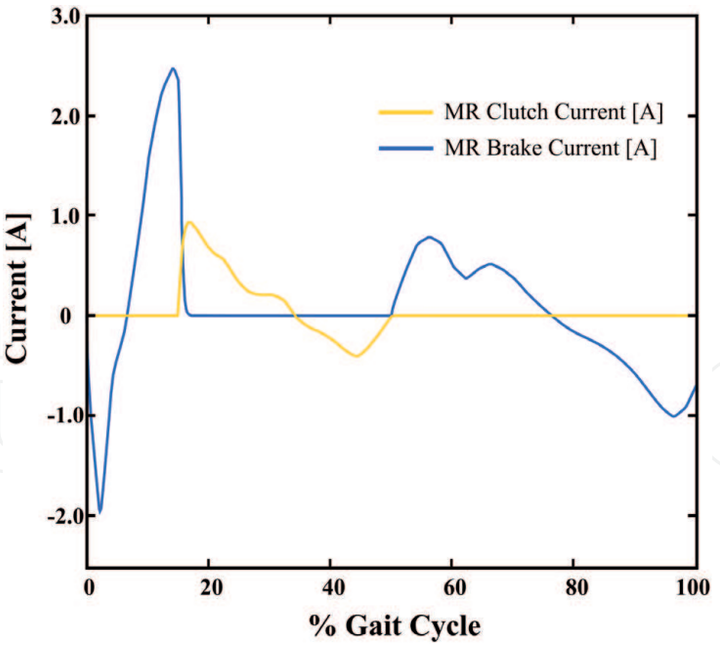

Figure 4.
Input current on the MR Clutch and MR Brake coils during the gait cycle.

Natural convection and radiation are also considered for the components whose surfaces are exposed to the air. The heat transfer coefficient, h_T, composed by radiation and natural convection, is given by:

$$h_T = h_c + h_r \tag{13}$$

where h_c is the natural convection coefficient and h_r is the heat radiation coefficient. Here we considered h_T = 9.7x10E-6 W/(mm^2 °C) [35].

3.3 FEM analysis

The 3D modeling of the AMRK is shown in **Figure 5**. Since the actuator presents an axisymmetric configuration, a part corresponding to 1/360 of the actuator was

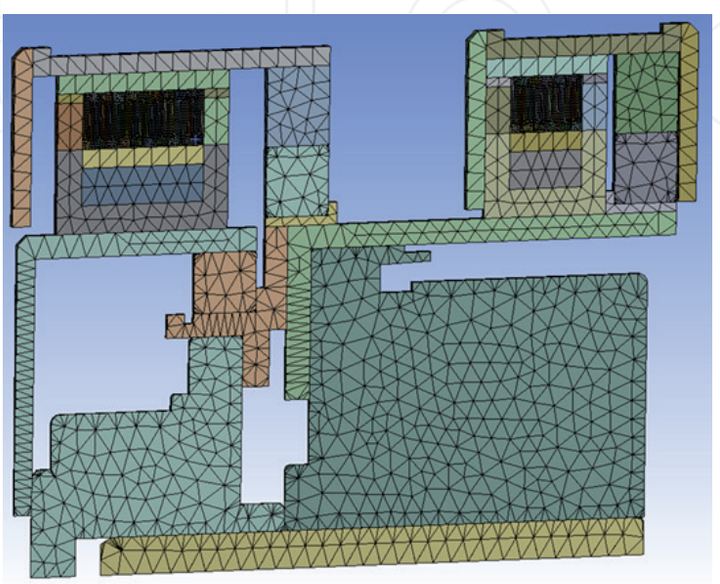

Figure 5.
AMRK Discretized model reduced to 1/360 to improve time processing.

Variable	Value
Motor heat generation	7.83E-6 W/mm^3
Harmonic drive heat generation	3.83E-5 W/mm^3
MR Brake coil heat generation	1.81E-4 W/mm^3
MR Clutch coil heat generation	2.22E-5 W/mm^3
Large bearings heat generation	3.98E-7 W/mm^3
Small bearing heat generation	4.51E-7 W/mm^3
MR fluid heat generation (MR brake)	1.03E-3 W/mm^3
Motor heat transfer coefficient[1]	1.72E-5 W/mm^2 °C
Heat transfer coef. remaining components[1]	9.70E-6 W/mm^2 °C

[1]*Room temperature = 25°C.*

Table 2.
Boundary conditions for the transient thermal analysis simulation.

simulated, to reduce the processing time. Unstructured tetrahedral elements were used for the model's mesh. Considering the dimensional differences of the actuator components, after a heuristic analysis of the actuator's mesh, different mesh sizes were adopted to obtain an acceptable precision of the results with reduced processing time. Mesh size for the MR fluid regions was 0.25 mm and for the other components we used mesh size of 2 mm.

To perform the transient thermal analysis, the AMRK is subjected to the operating modes presented in **Figure 1(d)** for 10,000 seconds, which represents 10.0 km walk, to reach the steady state condition. In such a simulation when the MU is activated, operating mode II, the EC motor, HD, MR clutch coil and bearings are the heat sources. When the MR brake is activated, operating mode I and III, the MR fluid and the brake coil and the larger bearings are the heat sources. The values of the boundary conditions are given in **Table 2**.

4. Results and discussion

After build the thermal model of the AMRK, we carried out a transient thermal analysis considering the actuator is subjected to over-ground walking for a long period of time. The initial temperature of the actuator and environment was 25°C. **Figure 6(a)** presents the temperature color map for the steady state condition and **Figure 6(b)** shows the temperature variation across time in each component of the actuator.

After 6000 s of simulation, which represents a 6.0 km walk, the AMRK reached the steady state temperature distribution, **Figure 6(b)**. The simulation ran up to 10,000 s, but no change in the temperature distribution was observed, as presented in **Figure 6(a)**. The MR fluid is considered the most sensible element of the actuator to temperature rise and must be carefully evaluated. Moreover, for safe operation, it is important that the temperature of the copper wire does not exceed 150°C and the actuator's housing surface temperature does not exceed 43°C, so it does not cause injury to the user [46].

The maximum temperature observed after the simulation time was 30.86°C in the MR fluid region of the MR brake. As previously mentioned, the MR brake works in full-slip condition and dissipate energy as heat in the MR fluid region. The full-slip operation is the most critical condition for heat generation in MR fluid-based

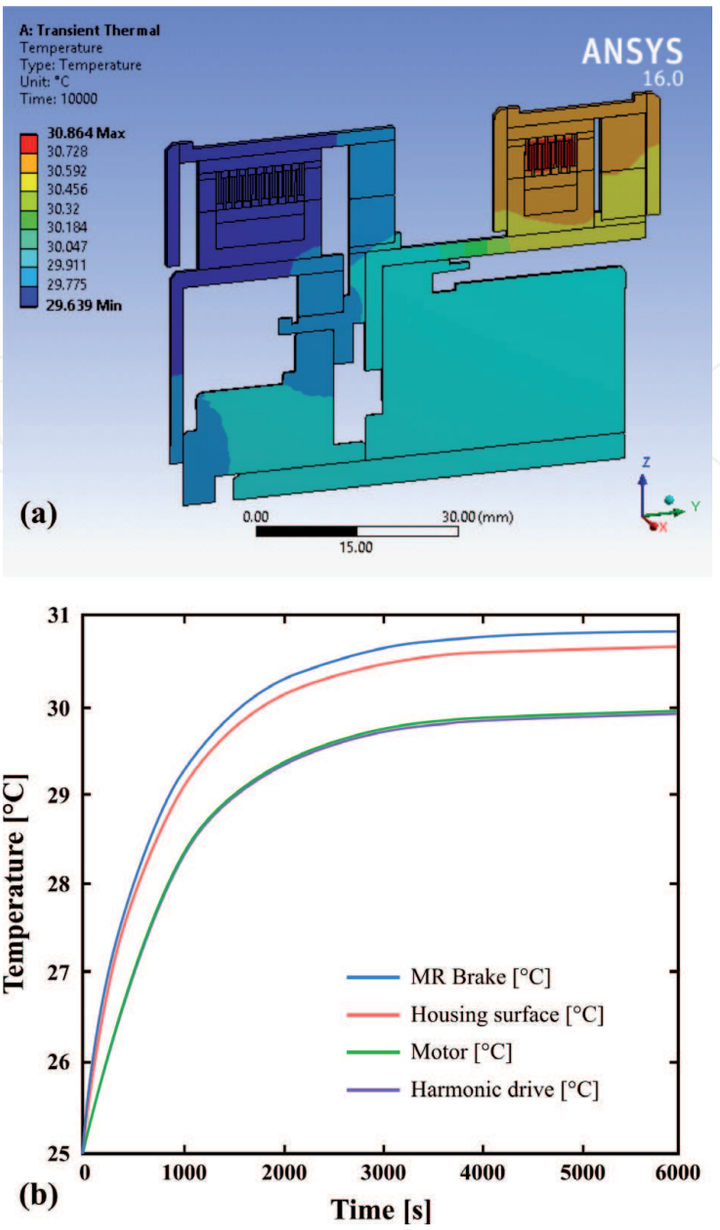

Figure 6.
Transient thermal analysis of the AMRK. (a) Temperature color map for steady state condition. (b) Temperature variation of actuator's components over time.

devices and can lead to critical temperatures [41]. However, unlike the common applications of shear transmissions, the proposed operating modes for the AMRK just activate the MR brake, which works in full-slip condition, when the knee is subjected to negative work, thereby reducing the heat generated. The MR clutch, as previously mentioned, works in non-slip condition and the heat is generated by Joule effect in the coil and not in the fluid area. Compared to previous applications of MR fluid-based transmissions, such as the shear transmission of Chen et al. [33] and the MR clutches proposed in Wang et al. [35, 41] and Leal-Junior et al. [36], where the temperature reached more than 120°C in full-slip condition, the temperature reached by the AMRK while working with the proposed operating modes, is not critical to the MR fluid integrity. On the other hand, from a braking torque control point of view, a more careful analysis should evaluate if this temperature increase can affect torque capacity of the MR brake. To improve the braking torque control in a rising temperature scenario a temperature-dependent shear stress, as proposed in [35], should be taken in to account.

The maximum temperature reached in the motor and harmonic drive was 29.94°C and 29.92°C, respectively, which are within the working limit temperature recommended by the supplier's catalog, up to 125°C and 120°C, respectively. The maximum temperature reached on the surface of the actuator was 30.68°C, which is not harmful to human skin [46]. These results validate the purpose usage of the AMRK as an actuator for knee replacement/assistance for over-ground walking.

5. Final remarks

This work presented the thermal analysis of the Active Magneto-Rheological Knee actuator (AMRK) for lower-limb prostheses and exoskeletons. The AMRK is composed by a motor unit (EC motor, harmonic drive, and MR clutch), responsible for generating positive work, that works in parallel to a MR brake, used to dissipate energy when the knee is subjected to negative work conditions. The proposed configuration is designed to perform a proper walk with low energy consumption [25, 26]. The thermal model for the components of the MR actuator was presented. EC motor, harmonic drive, MR clutch, MR brake, and bearings were modeled to assess the thermal behavior of the knee when subjected to a long walk over the ground. The results indicate that the proposed operating modes are effective to avoid actuator overheating. The maximum temperatures reached in each component are within the tolerances established by the suppliers and no damage is caused to the system, as well as to the MR fluid. The external steady state temperature of the actuator is about 31°C, which does not represent risk for the user. Future work will consider evaluating the temperature of the system under more severe working conditions, such as going up and down stairs.

Acknowledgements

This research was partially funded by grants from FAPES (Fundação de Amparo à Pesquisa e Inovação do Espírito Santo) TO 0480/2015 Project No. 67637574/15, TO 207/2018 Project No. 83276262, and TO 151/2021 Project No. 2021-8GJZ6. The authors honor Marcos Pinotti (in memoriam) for his important contribution to this work.

Conflict of interest

The authors declare that there is no conflict of interest.

Author details

Rafhael Milanezi de Andrade[1,2*], André Palmiro Storch[1], Lucas de Amorim Paulo[1], Antônio Bento Filho[1], Claysson Bruno Santos Vimieiro[2,3] and Marcos Pinotti[2]

1 Laboratory of Robotics and Biomechanics, Department of Mechanical Engineering, Universidade Federal do Espírito Santo, Vitória, ES, Brazil

2 Bioengineering Laboratory, Department of Mechanical Engineering, Graduate Program in Mechanical Engineering, Universidade Federal de Minas Gerais, Belo Horizonte, MG, Brazil

3 Graduate Program in Mechanical Engineering, Pontifícia Universidade Católica de Minas Gerais, Belo Horizonte, MG, Brazil

*Address all correspondence to: rafhaelmilanezi@gmail.com

References

[1] Cappozzo A, Figura F, Gazzani F, Leo T and Marchetti M, Angular displacements in the upper body of AK amputees during level walking Prosthet. Orthot. Int. 6 131-8, 1982.

[2] Fatone S, Stine R, Gottipati P and Dillon M, Pelvic and spinal motion during walking in persons with transfemoral amputation with and without low back pain Am. J. Phys. Med. Rehabil. 95 438-47, 2016.

[3] Bogue, R., Robotic exoskeletons: a review of recent progress, Industrial Robot: An International Journal, V. 42, n. 1, p. 5 – 10, 2015.

[4] Pieringer, D. S., Grimmer, M., Russold, M. F. and Riener, R. "Review of the actuators of active knee prostheses and their target design outputs for activities of daily living," Jul. 2017.

[5] Andrade RM, Bento Filho A, Vimieiro CBS, and Pinotti M (2018) Optimal design and torque control of an active magnetorheological prosthetic knee. Smart Materials and Structures 27:105031.

[6] Martinez-Villalpando. E. C., Her, H., 2009, Agonist-antagonist active knee prosthesis: A preliminary study in level-ground walking, J.Rehabilitation Res. Development, 46, 361-374;

[7] Lauwerys, C., Swevers, J. and Sas, P., 2002, Linear control of car suspension using nonlinear actuator control, Proceedings do ISMA2002, Leuven-Bélgica;

[8] Geng, Y., Yang, P., Xu, X., Chen, L., 2012 Design and simulation of Active Transfemoral Prosthesis. 24th Chinese Control and Decision Conference (CCDC). p. 3724-3728.

[9] Andrade RM and Bonato P (2021) The Role Played by Mass, Friction, and Inertia on the Driving Torques of Lower-Limb Gait Training Exoskeletons. IEEE Transactions on Medical Robotics and Bionics, V. 3, n. 1, pp. 125-136, Feb. 2021. doi: 10.1109/TMRB.2021.3052014.

[10] Filho, A. B., Andrade, R. M., Matos, M. C., 2014, Digital Prototyping of a Series Elastic Actuator for Exoskeletons, CONEM 2014;

[11] Garcia, E., Arevalo, J. C., Munoz, G., 2011, On the biomimetic design of agile-robot legs. Sensors, Basel, Switzerland, 11, 11305;

[12] Leal-Junior, A. G. ; Andrade, R. M. ; Bento Filho, A. Series Elastic Actuator: Design, Analysis and Comparison. Recent Advances in Robotic Systems. 1ed., InTech, p. 203-234, 2016a.

[13] Fiorezi, GG.; Moraes, JS.; Ulhoa, PHF.; Andrade, RM Biomimetic Design of a Planar Torsional Spring to an Active Knee Prosthesis Actuator Using FEM Analysis, Proceedings 2020, V. 64, n. 1:30. Doi: 10.3390/IeCAT2020-08505.

[14] Leal-Junior, A. G. ; Andrade, R. M. ; Bento Filho, A., Linear Serial Elastic Hydraulic Actuator: Digital Prototyping and Force Control, IFAC-PapersOnLine, 48 (6), 2015, 279-285.

[15] Vicente, J. De, Klingenberg, D.J., Hidalgo-Alvarez, R. Magnetorheological fluids: a review. Soft Matter, v. 7, p. 3701-3710, 2011.

[16] Leal-Junior, A. G., Campos, V., Díaz, C., Andrade, R. M., Frizera, A., Marques, C., A machine learning approach for simultaneous measurement of magnetic field position and intensity with fiber Bragg grating and magnetorheological fluid, Optical Fiber Technology, V. 56, 2020, 102184.

[17] Yang, G., 2001, Large-scale magnetorheological fluid damper

for vibration mitigation: modeling, testing and control, PhD Dissertation University of Notre Dame, Indiana, USA.

[18] Sung, K. G., and Choi, S. B., 2008, Effect of an electromagnetically optimized magnetorheological damper on vehicle suspension control performance, Proc. Inst. Mech. Eng., 222, 2307-19;

[19] Kavlicoglu, B. M., Gordaninejad, F., Evrensel, C., Fuchs, A. and Korol, G., 2006, A semi-active magnetorheological fluid limited slip differential clutch, Trans. ASME, J. Vib. Acoust., 128, 604-10;

[20] Nguyen, Q. H. and Choi, S. B., 2010, Optimal design of an automotive magnetorheological brake considering geometric dimensions and zero-field friction heat, Smart Mater. Struct., 19, 115024;

[21] Takashi, T., Sano, A., 2005, Fully Adaptive Vibration Control for Uncertain Structure Installed with MR Damper , American Control Conference, 2005. Proceedings of the 2005, 7, 4753 – 4759;

[22] Carlson, J. D., Matthis, W. and Toscano, J. R., 2001, Smart prosthetics based on magnetorheological fluids, Proc. SPIE, 4332, 308-16;

[23] Dong, S. F., Lu, K. Q., Sun, J. Q. and Rudolph, K., 2005, Rehabilitation device with variable resistance and intelligent control, Med. Eng. Phys., 27, 249-55;

[24] Dong, S. F., Lu, K. Q., Sun, J. Q. and Rudolph, K., 2006, A prototype rehabilitation device with variable resistance and joint motion control, Med. Eng. Phys., 28, 348-55;

[25] Andrade RM, Martins, JSR., Pinotti M, Bento Filho A and Vimieiro CBS (2021) Novel active magnetorheological knee prosthesis presents low energy consumption during ground walking. Journal of Intelligent Material Systems and Structures. doi:10.1177/1045389X20983923

[26] M. Andrade, A. B. Filho, C. B. S. Vimieiro and M. Pinotti, "Evaluating Energy Consumption of an Active Magnetorheological Knee Prosthesis," 2019 19th International Conference on Advanced Robotics (ICAR), Belo Horizonte, Brazil, 2019, pp. 75-80, doi: 10.1109/ICAR46387.2019.8981642

[27] Chen, J. Z.; Liao, W. H., 2006, A leg exoskeleton utilizing a magnetorheological actuator. Proceedings of IEEE International Conference on Robotics and Biomimetics. p. 824-829.

[28] Bento-Filho A, Tonetto CP, Andrade RM (2021) Four legged Guará robot: from inspiration to implementation, Journal of Applied and Computational Mechanics. doi:10.22055/JACM.2021.35212.2613.

[29] Andrade RM, (2018) Joelho magneto-reológico para próteses transfemurais: prototipagem digital, fabricação e identificação experimental. Doctoral Thesis, Federal University of Minas Gerais, Belo Horizonte, May 2018. Available: https://repositorio.ufmg.br/handle/1843/BUBD-AZ2MNM.

[30] Andrade RM, Bento Filho A, Vimieiro CBS, and Pinotti M (2016) Atuador magneto- reológico para próteses, exoesqueletos e outras aplicações robóticas e uso. BR Patent Application BR102016024912A2.

[31] Kowol, P., Pilch, Z., 2015, Analysis of the magnetorheological clutch working at full slip state, PRZEGLĄD ELEKTROTECHNICZNY, 91, 108-111.

[32] Andrade, R. M., Paulo, L. A., Bento Filho, A., Vimieiro, C., 2017. Transient Thermal Analysis of a MR Clutch for Knee Prostheses and Exoskeletons,

in: Procceedings of the 24th ABCM International Congress of Mechanical Engineering. https://doi.org/10.26678/ABCM.COBEM2017.COB17-0311

[33] Chen, S., Huang, J., Jian, K., Ding, J., 2015, Analysis of Influence of Temperature on Magnetorheological Fluid and Transmission Performance, Advances in Materials Science and Engineering, 2015, 1-7.

[34] Wang, D., Zi, B., Zeng, Y., Hou, Y., Meng, Q., 2014, Temperature-dependent material properties of the components of magnetorheological fluids, J Mater Sci, 49, 8459-8470.

[35] Wang, D., Zi, B., Zeng, Y., Xie, F., Hou, Y., 2015, An investigation of thermal characteristics of a liquid-cooled magnetorheological fluid-based clutch, Journal of Smart Materials and Strutures, 24, 1-13.

[36] Leal-Junior, A. G. ; Andrade, R. M. ; Bento Filho, A. Transient Thermal Analysis Of A Magnetorheological Clutch. In: 16th Brazilian Congress of Thermal Sciences and Engineering - ENCIT 2016b.

[37] Zipster, L., Richter, L., Lange, U., 2001, Magnetorheologic fluids for actuators, Sensors and Actuators A, 92, 318-325.

[38] Rossa, C., Jaegy, A., Lozada, J., Micaelli, A. Design Considerations for Magnetorheological Brakes. IEEE/ASME Transactions on Mechatronics, v. 19, p. 1669-1680, 2014. DOI: 10.1109/TMECH.2013.2291966

[39] Andrade RM, Sapienza S, and Bonato P (2019b) Development of a "transparent operation mode" for a lower-limb exoskeleton designed for children with cerebral palsy. IEEE International Conference on Rehabilitation Robotics (ICORR). 512-517. doi:10.1109/ICORR.2019.8779432.

[40] Guo, H. T., and Liao, W. H., 2012, A novel multifunctional rotary actuator with magnetorheological fluid, Smart Mater. Struct., 21, 065012, (9pp);

[41] Wang D and Hou Y 2013 Design and experimental evaluation of a multidisk magnetorheological fluid actuator J. Intell. Mater. Syst. Struct. 24 640-50.

[42] Maxon DC motor and maxon EC motor Key information. Maxon Group. Available in: https://www.maxongroup.com/medias/sys_master/8815460712478.pdf?attachment=true

[43] Cengel, Y. A., 2002, Heat Transfer: A Practical Approach, Second Edition. McGraw-Hill.

[44] Craiu, O., Machedon, A., Tudorache, T., Morega, M., Modreanu, M., 2010, 3D Finite Element Analysis of a Small Power PM DC Motor, 12th International Conference on Optimization of Electrical and Electronic Equipment;

[45] NTN Ball and Roller Bearings (Cat. No. 2203/E), NTN Corporation. Available in: https://www.ntnglobal.com/en/products/catalog/en/2203/index.html

[46] Moritz, A. R., Henriques Jr., F. C., 1947, Studies of termal injuries: II The relative importance of time and surfasse temperature in the causation of cutaneous burns. AM J Pathol; 23:695-720.